Validation of FAST.Farm Against Large-Eddy Simulations

J Jonkman, P Doubrawa, N Hamilton, J Annoni and P Fleming

National Renewable Energy Laboratory, Golden, CO 80401, USA

E-mail: jason.jonkman@nrel.gov

Abstract. FAST.Farm is a new midfidelity, multiphysics engineering tool for modeling the power performance and structural loads of wind turbines within a wind farm, including wake and array effects. Previous calibration of the tuneable model parameters of FAST.Farm has shown that its prediction of wake dynamics for a single wind turbine across different atmospheric stability conditions and nacelle-yaw errors matches well with high-fidelity large-eddy simulation at a small fraction of the computational expense. This paper presents a validation of FAST.Farm against large-eddy simulation for a series of cases—independent from those used to support the calibration—considering single-turbine and small wind-farm scenarios, which are both subject to variations in inflow and control. The validation has demonstrated that FAST.Farm reasonably accurately predicts: (1) thrust and power for individual turbines both in isolation and down the row of the small wind farm, (2) wake meandering behavior across different atmospheric conditions, and (3) averaged wake-deficit advection, evolution, and merging effects. The validation also highlights potential physics that could be improved in FAST.Farm in the future.

1. Introduction

FAST.Farm is a new midfidelity, multiphysics tool developed by the National Renewable Energy Laboratory (NREL) that is applicable to engineering problems in research and industry involving wind farm optimization. This tool aims to address the current underperformance, failures, and expenses in the wind industry [1]. Achieving wind cost-of-energy targets requires improvements in wind farm performance and reliability and reduced uncertainty and expenditures, which has been eluded by the complicated nature of the wind farm design problem. FAST.Farm aims to accurately model the relevant physics for predicting power performance and structural loads and maintain low computational costs to support a highly iterative and probabilistic design process and systemwide optimization.

This paper presents a validation of FAST.Farm against high-fidelity simulation results from NREL's large-eddy simulation (LES) model known as the Simulator fOr Wind Farm Applications (SOWFA) [2] for a series of cases involving a single turbine and small wind farm, both of which are subject to variations in inflow and control. In previous work [3], a series of high-fidelity SOWFA simulations were conducted to support the calibration of FAST.Farm. The validation cases presented in this paper complement the calibration process by considering modest variations in inflow and control from those used in the calibration. The FAST.Farm simulations are run without modifications to the default model parameters derived from the calibration work to check their robustness and range of applicability. The results aim to highlight where FAST.Farm functions well and where potential improvements could be required in the future. SOWFA has been validated in prior work, e.g. in [4]; although no numerical simulation is perfect, the SOWFA solutions are taken as the benchmark in the FAST.Farm calibration and validation effort. Further validation of FAST.Farm against high-fidelity simulations involving other operational conditions, larger wind farms, and experimental data will take place in the future. Future

applications of FAST.Farm are expected to involve a synergistic relationship with SOWFA (or equivalent) in a multifidelity modeling framework wherein high-fidelity simulations will be used to calibrate FAST.Farm for a subset of cases and FAST.Farm will be run many times to support the analysis required by the application.

2. Approach and methods

An overview of FAST.Farm, SOWFA, and the calibration of FAST.Farm are given in the upcoming subsections, followed by a description of the new validation cases and the simulation setups.

2.1. Overview of FAST.Farm and SOWFA

FAST.Farm is a nonlinear, dynamic, multiphysics engineering tool composed of multiple submodels, each representing different physics domains of the wind farm. FAST.Farm uses NREL's OpenFAST tool (formerly known as FAST) to solve the aero-hydro-servo-elastic dynamics of each individual turbine but considers additional physics for ambient wind across the wind farm in the atmospheric boundary layer; a wind farm super controller; and wake deficits, advection, deflection, meandering, and merging. FAST.Farm is based on the principles of the dynamic wake meandering (DWM) model [5] but addresses many of the limitations of previous DWM implementations. The main idea behind DWM is to capture key wake features pertinent to accurate wind farm simulation—including the wake-deficit evolution, which is important for performance, and wake meandering, which is important for structural loads—while maintaining computational efficiency. Rotor aerodynamics in FAST.Farm are modeled with blade-element momentum theory (with advanced corrections) and wake dynamics are modeled with an engineering implementation of wake evolution based on the thin shear-layer approximation of Navier-Stokes, wake meandering is modeled as a passive tracer, and wake merging is modeled via superposition. The FAST.Farm solution is solved serially or in parallel using Open Multi-Processing (OpenMP), with full wind farm simulations essentially running in real time (when using at least one core per turbine). Details on the theoretical basis and implementation of FAST.Farm are explained in [1]. Unique innovations in FAST.Farm not found in previous DWM implementations include:

- The use of LES-generated precursors for ambient wind throughout the wind farm
- New models for wake advection, deflection, and merging
- The inclusion of a super controller
- The ability to solve all wind turbines together with optional parallelization
- The calibration of model parameters against high-fidelity LES.

SOWFA is an LES tool that incorporates OpenFAST through an advanced actuator-line method (ALM) to predict wind farm performance and loads, relying on high-performance computing with high resource demand. SOWFA directly resolves the large, energy-containing scales of turbulence and wake dynamics [2]. These computations require up to 1 billion mesh cells and days to weeks of computing time per simulation, relegating the application of SOWFA to very few simulations, which is impractical for engineering design.

2.2. Calibration of FAST.Farm against SOWFA

The calibration procedure involved iteratively comparing the outputs of FAST.Farm to those from SOWFA for a set of calibration cases involving a single NREL 5-MW reference wind turbine [6] subject to variations in inflow for different atmospheric stability conditions and variations in wind turbine operation (including nacelle-yaw error and transient events), combined with an optimization algorithm to ensure that the tunable model parameters of FAST.Farm are set adequately so as to accurately model wind turbine wake dynamics. Both FAST.Farm and SOWFA use the same LES-generated precursor simulations to derive their ambient wind inflow, enabling a direct comparison of wake response between FAST.Farm and SOWFA with only a limited set of SOWFA simulations run (nine in total). Several methods have been developed and assessed for extracting the wake-deficit profile and the meandering wake centerline dependent on downwind distance from each SOWFA simulation, providing a robust

way of quantifying the wake behavior in a meandering frame of reference so it can be directly compared to the results predicted by FAST.Farm [7].

The calibration of FAST.Farm against SOWFA simulations was used to finalize the default model-calibration parameters of FAST.Farm and has demonstrated that FAST.Farm accurately captures (1) the change in wake-deficit evolution with downstream distance (with a slight overprediction of wake deficit for unstable conditions and large nacelle-yaw errors) and (2) the overall wake-meandering statistics across different atmospheric stability conditions (with a slight overprediction of vertical mean deflection and underprediction of variations about the mean for stable conditions). Details on the calibration methodology and results are presented in [3].

2.3. Validation cases

To support the initial validation of FAST.Farm, six additional SOWFA and FAST.Farm simulations were run—independent from those used to support the calibration—involving a single NREL 5-MW baseline turbine [6] and small wind farm of three of these turbines subject to variations in inflow and control, as summarized in table 1. Each case in table 1 represents a modest change to equivalent cases ran for the calibration, including:

- A change to the mean wind speed and turbulence intensity (TI) (case V6_TI8_1WT at 6 m/s and 8% TI compared to neutral calibration case "N" at 8 m/s and 10% TI from [3])
- A change to the nacelle-yaw error (case V8_TI10_1WT_Yaw at 15° compared to calibration cases "N_{+10}" and "N_{+25}" at 10° and 25°, respectively)
- A change to the TI and shear with yaw error (case V8_TI5_1WT_Yaw at 6% TI and a 0.1 power-law shear exponent compared to calibration case "N_{+10}" at 10% TI and 0.2 shear)
- The addition of downstream turbines for a small wind farm consisting of a single row of three NREL 5-MW wind turbines spaced 8 rotor diameters (D) apart with the mean flow aligned down the row (cases V8_TI10_3WT, V8_TI10_3WT_Yaw and V8_TI6_3WT compared to the single turbine calibration cases "N", "N_{+10}"/"N_{+10}"/"N" and stable case "S", respectively). Case V8_TI10_3WT_Yaw is meant to represent a small wind farm with a wake steering controls strategy.

Table 1. Validation cases.

Case	Number of turbines	Turbine spacing	Mean hub-height wind speed	Turbulence intensity	Shear exponent	Yaw error
V6_TI8_1WT	1	-	6 m/s	8%	0.2	0°
V8_TI10_1WT_Yaw	1	-	8 m/s	10%	0.2	15°
V8_TI6_1WT_Yaw	1	-	8 m/s	6%	0.1	10°
V8_TI10_3WT	3	8D	8 m/s	10%	0.2	0°
V8_TI10_3WT_Yaw	3	8D	8 m/s	10%	0.2	10°/10°/0°
V8_TI6_3WT	3	8D	8 m/s	6%	0.1	0°

2.4. Simulation setup

The ambient inflow for the six validation cases in table 1 was prescribed from three unique LES-generated freestream precursors at

- 6 m/s mean hub-height wind speed, 8% TI, and a power-law shear exponent of 0.2
- 8 m/s, 10% TI, and a shear of 0.2
- 8 m/s, 6% TI, and a shear of 0.1.

Each of these three precursors was generated in SOWFA (without wind turbines/ALM) on a $X \times Y \times Z$ = 5-km × 2-km × 350-m domain with a uniform spatial resolution of 10 m, a time length of 2,000 s, and mean streamwise flow propagating along X. The freestream precursor flow fields are then used as

inflow for the six FAST.Farm and SOWFA simulations with wind turbines and wakes. For the FAST.Farm simulations, this freestream flow across the spatial domain is saved with a temporal resolution of 2 s for the large, low-resolution (full wind farm) domain and at 1/3 s for the small, high-resolution domains around each rotor. Although some cases in the calibration effort from [3] considered stable atmospheric conditions (including buoyancy effects from thermal gradients), the LES-generated precursors in this validation effort approximate stable stratification by varying the bottom-wall roughness and therefore the turbulence intensity and shear. This was done to circumvent the computationally demanding simulation of stable atmospheric conditions (and the consequent small turbulent length scales), which require small time steps and fine spatial resolution.

Each case in table 1 is simulated with wind turbines and wakes in both FAST.Farm and SOWFA for 1,800 s (30 min), after elimination of a 200-s start-up transient (as was done for the calibration work in [3]). The FAST.Farm simulations are run without modifications to the default model parameters derived from the calibration work to check their robustness and range of applicability. The wake discretization in FAST.Farm consists of 140 wake planes per rotor, each with a radial finite-difference grid of 40 radial nodes. The SOWFA-ALM simulations use the same spatial domain as the precursor simulations, but with two inner refinement zones of 5 m and 2.5 m resolution around and downstream of each rotor, respectively. While SOWFA has been interfaced to OpenFAST for modeling the coupled aero-hydro-servo-elastic dynamics of each individual turbine, the interface to OpenFAST has been disabled for this validation effort; instead, the rotors are modeled with a rigidly rotating ALM with a variable generator speed as the only structural degree of freedom (DOF) (along with the associated generator torque controller). To mimic this simplification, all structural DOFs except the generator DOF were disabled in OpenFAST for the FAST.Farm simulations. The wind turbine properties match those of the NREL 5-MW baseline turbine [6], with the exception of the structural rigidity and a rotor tilt that has been set to zero degrees. Further validation of blade, drivetrain, and tower excitation, dynamics, and loading will take place in the future. Each SOWFA-ALM simulation took on the order of 2 days to run in parallel mode with 600 cores, whereas each FAST.Farm case took on the order of a few hours to run in serial mode on a single core. The computational expense of FAST.Farm is heavily driven by file reading and writing; with the LES precursor data to be read into FAST.Farm stored locally, little flow visualization data written as output, and parallel mode utilized, the FAST.Farm solution will run faster than real time.

3. Results

The wind velocity output from FAST.Farm is processed at uniform 10-m and 2-s sampling resolution; SOWFA is processed at a 10-m and 1-s sampling resolution. The FAST.Farm and SOWFA results are compared qualitatively in terms of instantaneous flow visualizations of wind velocities on planes slicing through the three-dimensional domain of the wind farm, including a horizontal *XY* plane at hub height, vertical *YZ* planes at various downstream distances from each wind turbine, and a vertical *XZ* plane through the tower centerline(s). The results are further compared quantitatively in terms of the time series and probability density functions (PDFs) (i.e., histograms) of the generator power and torque and aerodynamic-applied rotor thrust and rotor speed for each wind turbine. Furthermore, the results are quantitatively compared in terms of azimuth and temporal averages of the axial and radial wake deficits in the meandering frame of reference, and time series and PDFs of the horizontal (*Y*) and vertical (*Z*) wake center positions at seven discrete YZ-planes downstream of each wind turbine between 2D and 8D in 1D intervals. These wake quantities are extracted consistently[1] from FAST.Farm and SOWFA at each downstream plane via the following steps (from [7]):

1) Estimate the vertical profile of freestream wind speed and use it to obtain velocity deficits
2) Identify the wake edge and wake center
3) Use the wake center to go from a fixed to a meandering frame of reference

[1]This approach to extracting wake quantities is consistent with the postprocessing method for SOWFA used in the calibration effort from [6]. But in [6], the wake quantities in FAST.Farm were output directly from FAST.Farm rather than by extracting information from the downstream planes.

4) Sample radial and axial flow deficits at various radial distances from the wake center to the edge at different azimuthal directions
5) Azimuthally and temporally average the sampled deficits.

For the small wind farm cases, the wind turbines are labeled as WT1, WT2, and WT3 from left (upstream) to right (downstream) in the subsequent discussion. Only a subset of the results are shown.

3.1. Flow visualizations

Instantaneous flow visualizations on the *XY* plane for cases V8_TI6_1WT_Yaw and V8_TI6_3WT are shown in figures 1 and 2, respectively. Outside of the wake region—especially outside of the refinement zones in SOWFA—the ambient flow is quite consistent between FAST.Farm and SOWFA, which results directly from the use of the same LES-generated precursors in both solutions. There are more differences within the refinement zones in SOWFA. Within the wake, general characteristics are consistent between FAST.Farm and SOWFA (e.g., the velocity deficits have similar magnitudes, the hub effect is clearly visible [because aerodynamic loads are only calculated on the blades] and the extent and direction of wake meandering are similar). However, SOWFA clearly has finer wake details because of the breakdown of vortices and wake-induced turbulence captured in SOWFA (but not in FAST.Farm), the refinement zones in SOWFA, and the axisymmetric-wake simplifications in FAST.Farm. In the FAST.Farm-generated *XY* planes, a discrete change in flow can be seen right at the plane of the rotor, which is a result of the wake propagation calculation for each wind turbine in FAST.Farm being initiated at the rotor plane. Conversely, SOWFA models the induction zone upstream of the rotor (aerodynamic induction is calculated by OpenFAST, but the upstream effect is not resolved in FAST.Farm). In the FAST.Farm-generated *XY* planes, one can also see small but discrete transitions in the flow at certain downstream distances (i.e., at approximately *X/D* = 12, 19, and 27 in figure 2). These transitions result from the discrete implementation of wake planes in FAST.Farm, where the wake is simply truncated at a given number of wake planes downstream (140 for the current simulations), where the wake deficit is suitably diminished.

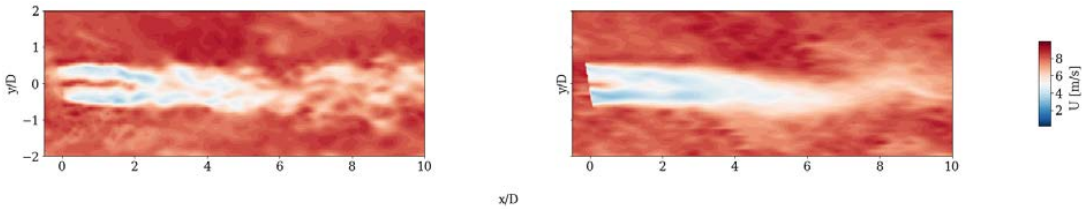

Figure 1. Instantaneous flow visualization on the *XY* plane from SOWFA (left) and FAST.Farm (right) for case V8_TI6_1WT_Yaw.

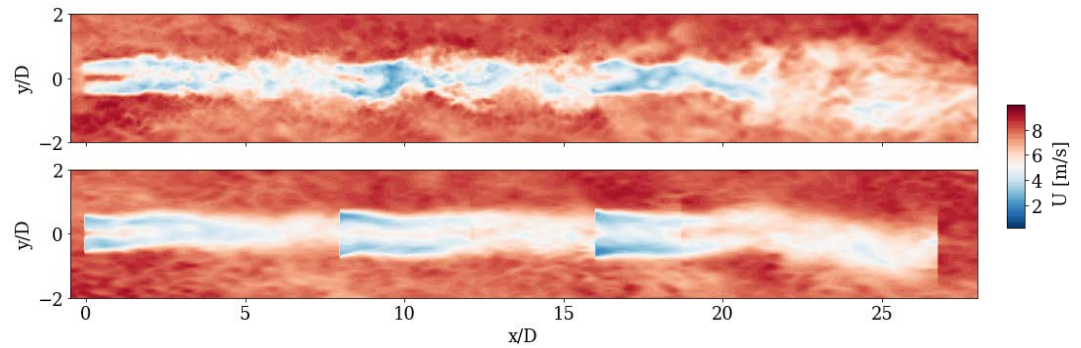

Figure 2. Instantaneous flow visualization on the *XY* plane from SOWFA (top) and FAST.Farm (bottom) for case V8_TI6_3WT.

Instantaneous flow visualizations on *YZ* planes 2D downstream from WT1 and WT2 for cases V8_TI10_3WT and V8_TI6_3WT are shown in figures 3 and 4, respectively. Again, the ambient flow is quite consistent between FAST.Farm and SOWFA outside of the wake. The wake behind WT1 is reasonably well-captured, but discrepancies in the wake increase after WT2 because of the added turbulence caused by the meandering wake impinging on the downstream rotors, especially for the wind farm case with lower ambient TI, where added turbulence is more important than the case with higher ambient TI.

3.2. Generator power and torque and rotor speed and thrust

Rotor thrust is the primary driver for wake deficits. As such, a consistent prediction of thrust between FAST.Farm and SOWFA is essential for a consistent prediction of wake and array effects. Time series and PDFs of the aerodynamic applied rotor thrust for cases V6_TI8_1WT and V8_TI10_3WT are shown

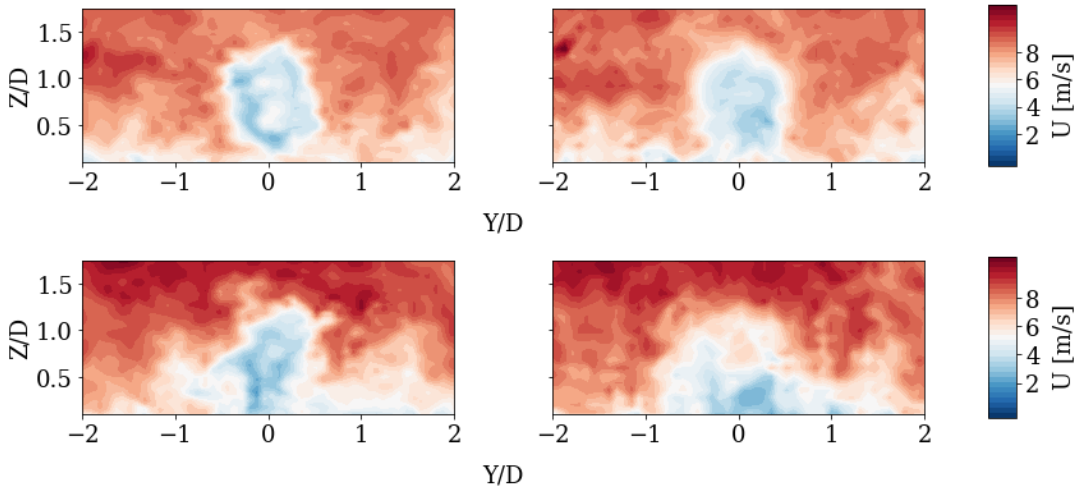

Figure 3. Instantaneous flow visualization on *YZ* planes 2D downstream from WT1 (top) and WT2 (bottom) from SOWFA (left) and FAST.Farm (right) for case V8_TI10_3WT.

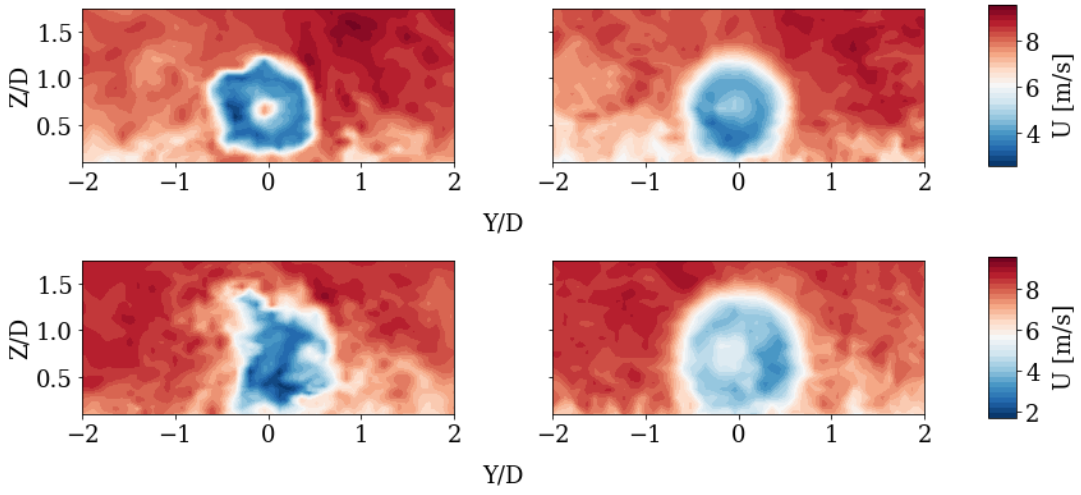

Figure 4. Instantaneous flow visualization on *YZ* planes 2D downstream WT1 (top) and WT2 (bottom) from SOWFA (left) and FAST.Farm (right) for case V8_TI6_3WT.

in figures 5 and 6, respectively. In general, the time series are quite consistent for the wind turbine (WT1) exposed to free-stream flow; for the downstream wind turbines (WT2 and WT3), there are a few oscillations in the time series that differ between FAST.Farm and SOWFA, likely because of the finer wake details and wake asymmetry captured by SOWFA when upstream wakes impinge on the downstream rotors. Statistically, the mean thrust compares reasonably well between FAST.Farm and SOWFA, with a small shift in the mean in most cases. The variation about the mean is shown to be reasonably consistent between FAST.Farm and SOWFA. FAST.Farm also captures the reduction in thrust for WT2 and WT3 relative to WT1 as a result of the lower wind speeds in the wake. In some of the cases, the thrust offsets between FAST.Farm and SOWFA could be related to the simulation setup in SOWFA. That is, the ALM in SOWFA uses a Gaussian spreading function to smooth the aerodynamic forces along an actuator line into body forces spread across several cells. The Gaussian width and accuracy of the method is dictated by the choice of the epsilon parameter [8]. In these SOWFA-ALM simulations, epsilon was chosen for numerical stability reasons (epsilon = 5 m) rather than for accuracy, and so the SOWFA simulations may be impacted by that choice.

Time series and PDFs of the generator power for cases V8_TI10_3WT and V8_TI10_3WT_Yaw are shown in figures 7 and 8, respectively. In general, the power matches reasonably well between FAST.Farm and SOWFA for the small wind farm without yaw error, including for the power loss for waked turbines downstream. As with the rotor thrust, there are small differences in the time series, but the statistical distribution matches reasonably well—while FAST.Farm underpredicts the mean generator power a bit down the row of turbines in the farm, the standard deviation about the mean and even the skewness of the distribution above the mean are captured by FAST.Farm. The offset between FAST.Farm and SOWFA in mean power for WT2 and WT3 is likely driven by an offset in the vertical mean wake deflection and a bit larger wake deficit in FAST.Farm (discussed more later). The skewness

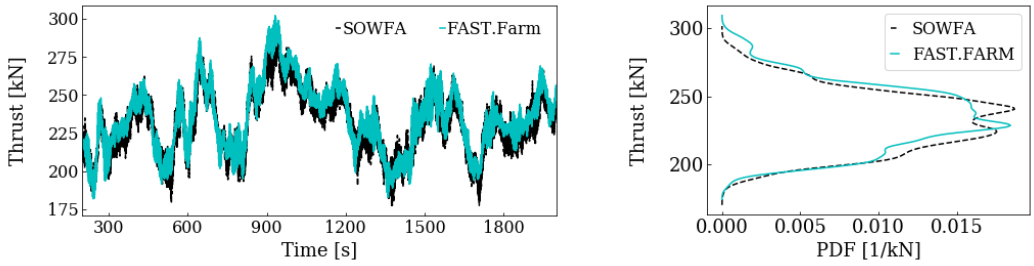

Figure 5. Time series (left) and PDF (right) of rotor thrust for case V6_TI8_1WT.

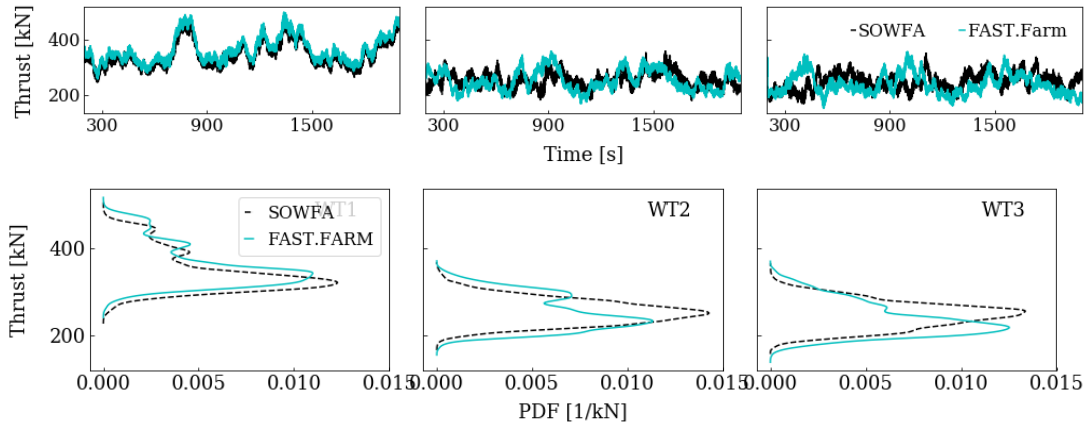

Figure 6. Time series (top) and PDFs (bottom) of rotor thrust for case V8_TI10_3WT.

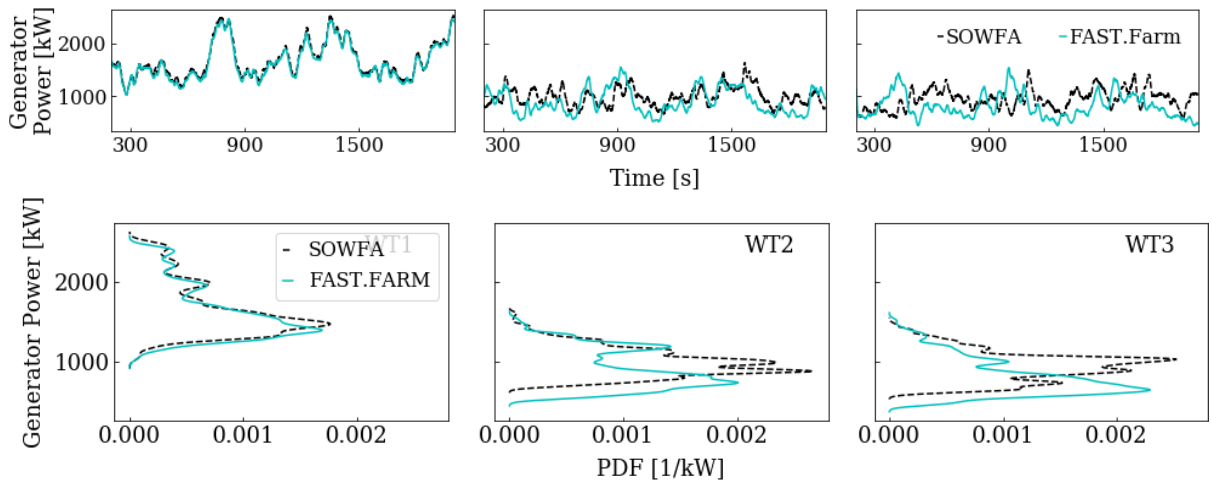

Figure 7. Time series (top) and PDFs (bottom) of generator power for case V8_TI10_3WT.

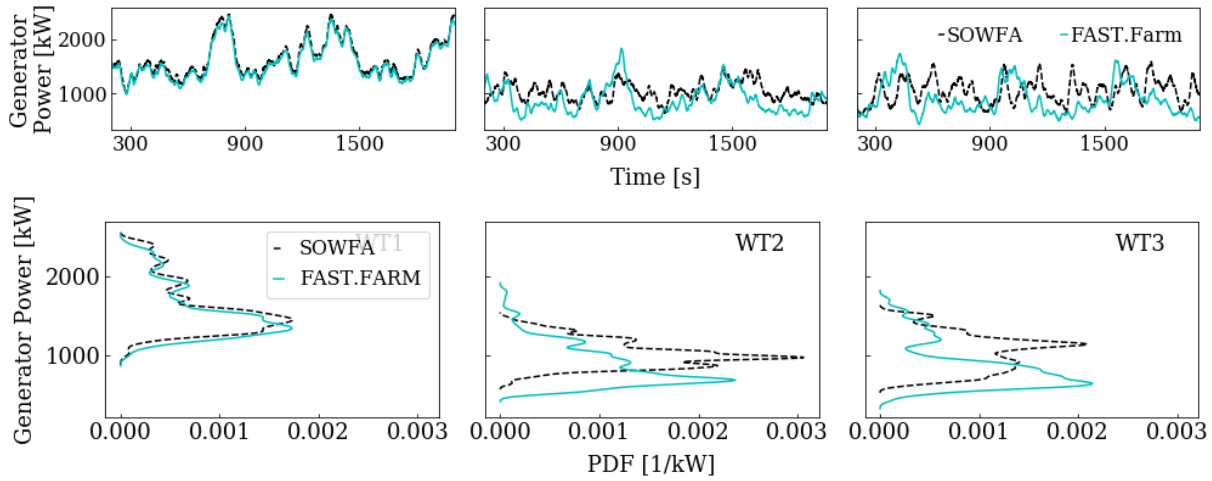

Figure 8. Time series (top) and PDFs (bottom) of generator power for case V8_TI10_3WT_Yaw.

of the variations about the mean towards higher generator powers is likely the result of the cubic relationship between wind speed and power, where the wind-speed gusts generate more power than is lost by wind-speed lulls. For the small wind farm with yaw errors for wake steering, a bit larger differences in power are found for WT2 and WT3, with a lower mean in FAST.Farm. This difference is likely due to the lack of a model for curled wakes in FAST.Farm under skewed-flow conditions. The generator-power PDFs are not as smooth as the rotor-thrust PDFs—likely due to the highly nonlinear relationship between generator power and wind speed—which implies a lack of statistical convergence that could be improved by running longer time-domain simulations in future FAST.Farm validation studies.

PDFs of the generator torque and rotor speed for case V8_TI10_3WT are shown in figure 9 and generally show the same trends as the thrust and power.

3.3. Wake meandering

Time series of the horizontal (*Y*) and vertical (*Z*) wake center positions between 2D and 8D downstream of the wind turbine in 2D intervals are shown in figure 10 for case V8_TI10_1WT_Yaw. While there is a small offset in the mean wake deflection in the vertical direction (discussed more later), in general, the time series of wake meandering is quite consistent with only minor features differing between FAST.Farm and SOWFA, likely because of the finer wake details and wake asymmetry captured by SOWFA. At times, numerical “spikes” are seen, which are likely the result of the wake-detection

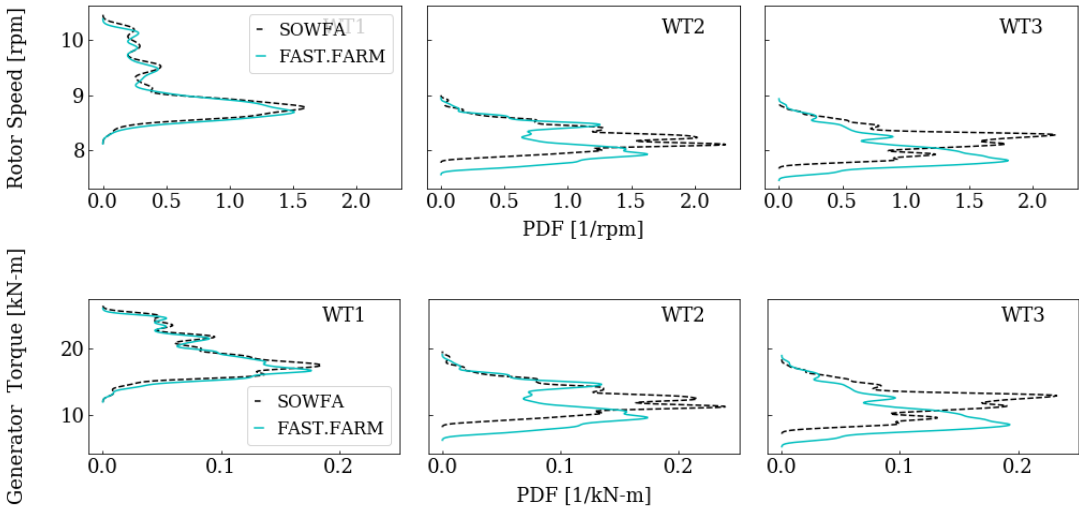

Figure 9. PDFs of rotor speed (top) and generator torque (bottom) for case V8_TI10_3WT.

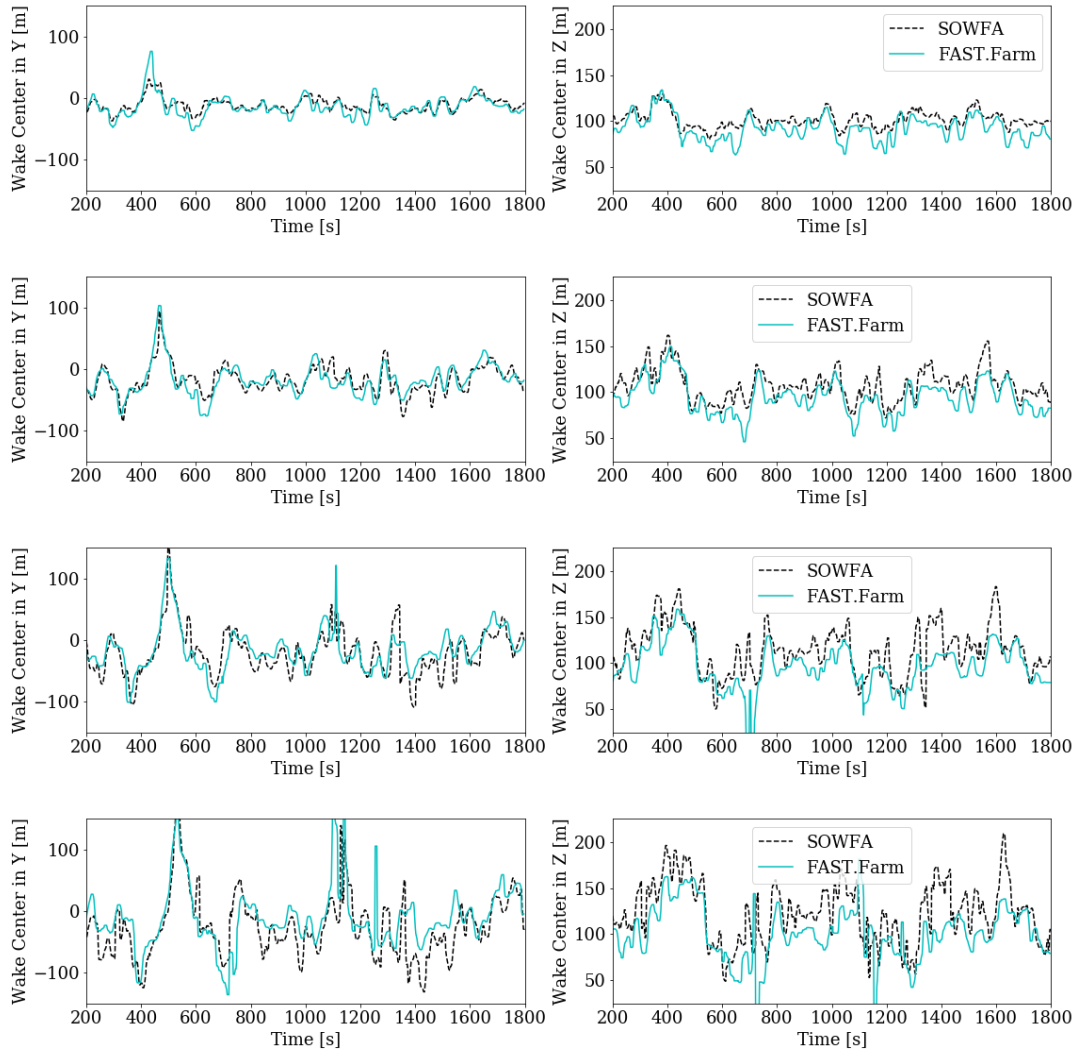

Figure 10. Time series of horizontal (left) and vertical (right) wake center positions between 2D to 8D downstream in 2D intervals (top to bottom) for case V8_TI10_1WT_Yaw.

algorithm [7] having a hard time locating the wake center when instantaneous wake deficits are small or highly asymmetric. When scanning the wake centers from 2D to 8D, the propagation of wake features downstream is clearly visible. This results from a combination of turbulence acting nearly frozen (although the turbulence is not considered frozen in either FAST.Farm or SOWFA) and an indication that the wake-advection speed in FAST.Farm—including the acceleration of the wake from near to far wake—is consistent with that of SOWFA.

PDFs of the horizontal (Y) and vertical (Z) wake center positions for cases V8_TI10_3WT and V8_TI6_3WT are shown in figures 11 and 12, respectively. PDFs are shown from 2D to 8D downstream of each wind turbine in 2D intervals, omitting the planes slicing through WT2 and WT3. The planes slicing through WT2 and WT3 are not shown because the wake propagation calculation for each wind turbine in FAST.Farm initiates discretely at the rotor plane, and so, the wake effects are not physically exact at these planes. Horizontally, the wake-meandering statistics are very consistent between FAST.Farm and SOWFA, with the largest deviation at a distance 2D downstream of WT1 for the case with lower ambient TI, where FAST.Farm predicts more meandering than SOWFA. Even deep behind WT3, the horizontal wake meandering is predicted quite well by FAST.Farm. Similar findings are observed for the vertical wake meandering, except that (1) the mean wake deflects lower with downstream distance in FAST.Farm than in SOWFA and (2) the wake meanders more in SOWFA than in FAST.Farm, both of which are exaggerated for the case with lower ambient TI. Without rotor tilt and the resulting skewed flow, the vertical mean wake deflection is likely driven by a combination of wind shear and the wake-induced boundary layer i.e flow speed-up around the wind turbines, the latter of

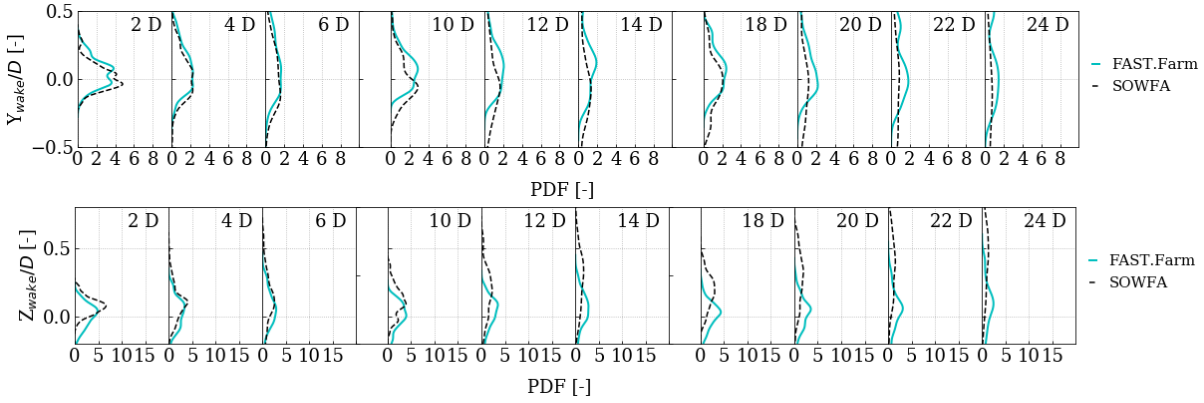

Figure 11. PDFs of the horizontal (top) and vertical (bottom) wake center positions for case V8_TI10_3WT.

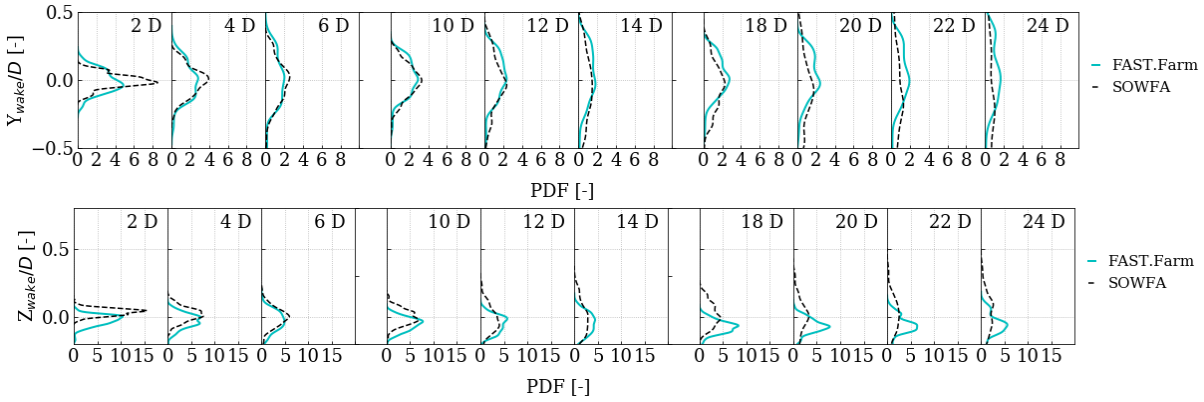

Figure 12. PDFs of the horizontal (top) and vertical (bottom) wake center positions for case V8_TI6_3WT.

which is not modeled in FAST.Farm. The more vertical wake meandering in SOWFA than FAST.Farm is likely driven by wake-induced turbulence not modeled in FAST.Farm, which is more important with lower ambient TI. Again, running longer simulations in the future would smooth out the PDFs and enable better comparisons between SOWFA and FAST.Farm.

3.4. Wake deficits

Radial profiles of the azimuth and temporal averages of the axial wake deficits in the meandering frame of reference from 2D to 8D downstream of each wind turbine in 2D intervals (neglecting the planes slicing through WT2 and WT3 for the same reason as discussed earlier) for cases V8_TI10_3WT and V8_TI6_3WT are shown in figures 13 and 14, respectively. The deficit is shown as the difference between the waked and ambient flow (and so a negative value indicates that the wind speed in the wake is less than in the freestream). As expected, the deficit is strongest at the wake center and decays with increasing radius (r), except in the near wake (2D), where the hub effect is visible in the case with lower ambient TI. Downstream of WT1, the wake deficits at a distance of 2D differ more between FAST.Farm and SOWFA than at distances further downstream. This is likely the result of the near-wake correction in FAST.Farm, which is targeted to produce accurate wake deficits in the far wake rather than accurately resolving the near wake. Further downstream, FAST.Farm clearly matches the wake-deficit evolution and recovery calculated by SOWFA on average. Downstream of WT2 and WT3, the wake deficits from FAST.Farm match well to SOWFA, but there are some notable differences. SOWFA does not predict a distinct hub effect at 2D for the case with lower ambient TI, which is likely the result of the averaging process smearing out the fine details and wake asymmetry predicted by SOWFA. The wake deficits are also a bit stronger in FAST.Farm compared to SOWFA for case V8_TI10_3WT. Regardless, figure 6 shows a lower rotor thrust in WT2 and WT3 compared to WT1, but the wake deficits do not change much downstream of WT2 and WT3 compared to WT1. This demonstrates that the wake merging model in FAST.Farm (based on a root-sum-square superposition locally at each point) is quite accurate under the conditions simulated.

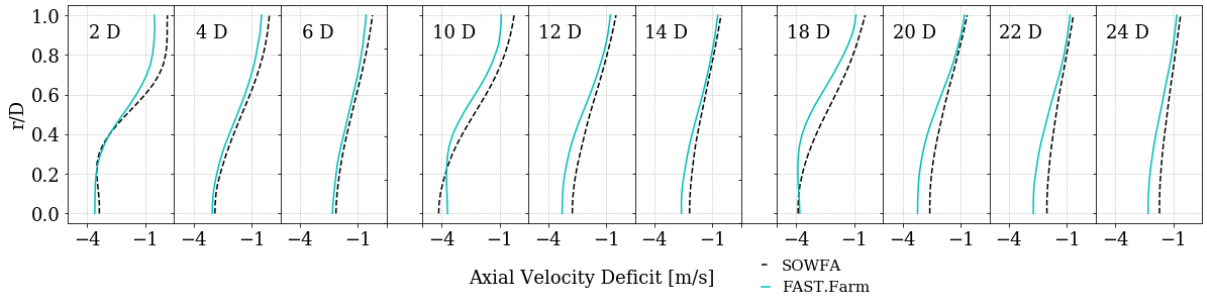

Figure 13. Axial wake deficits in the meandering frame of reference for case V8_TI10_3WT.

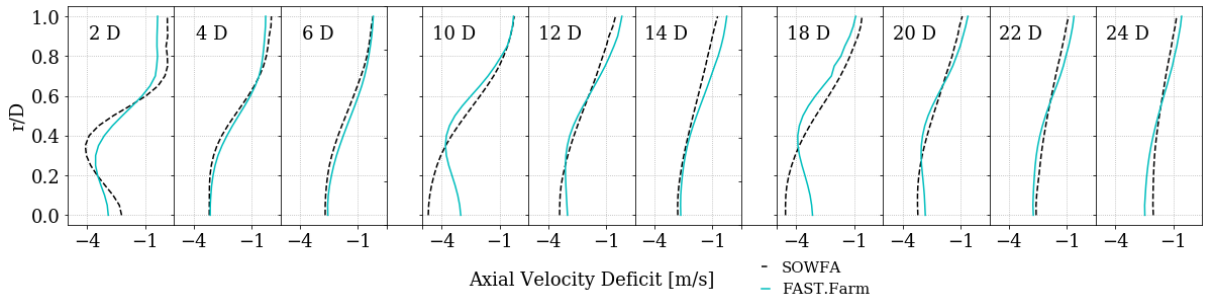

Figure 14. Axial wake deficits in the meandering frame of reference for case V8_TI6_3WT.

4. Conclusions

The new midfidelity, multiphysics wind farm engineering tool FAST.Farm has been validated against high-fidelity LES results from SOWFA for a series of cases—independent from those used to support the calibration—considering single-turbine and small wind-farm scenarios, both subject to variations in inflow and control. The default model parameters in FAST.Farm were derived from the calibration work and used for the validation to check their robustness and range of applicability. The results have shown that FAST.Farm functions reasonably well when predicting:

- The statistical distribution of generator power and torque and rotor thrust and speed for individual turbines, both in isolation and down a row of a small wind farm involving wake losses
- The time series and statistical distribution of horizontal and vertical wake meandering
- The azimuthally and temporally averaged wake-deficit advection, evolution, and merging, especially in the far wake.

Potential physics that could be improved in FAST.Farm in the future include predictions of:

- Finer wake details and wake asymmetry
- Near-wake effects (e.g., vortex breakdown)
- Wake-added turbulence, which is most important for cases with low ambient TI
- Wake-induced boundary layers and flow speed-up around the wind turbines, which impact the vertical wake deflection
- Curled wakes under skewed-flow conditions.

The ability to perform a large number of load-resolving simulations for the entire wind farm in a multistep design and optimization process that considers the full range of operational conditions is critical to future wind farm design. FAST.Farm was developed to meet this need. It is envisioned that FAST.Farm will create a paradigm shift in wind farm design capability, with potential future applications in reducing wind farm underperformance and loads uncertainty, developing wind farm controls to enhance the operation of existing wind farms, optimizing the siting and topology optimization of new wind farms, and innovating the design of wind turbines for the wind farm environment.

Further validation of FAST.Farm against high-fidelity simulations will involve longer simulations and coupling to wind turbine aero-hydro-servo-elastics to validate blade, drivetrain, and tower excitation, dynamics, and loading. Further validation against high-fidelity simulations for other operational conditions, larger wind farms, and experimental data will also take place in the future. Future applications of FAST.Farm are expected to involve a synergistic relationship with SOWFA (or equivalent) in a multifidelity modeling framework where high-fidelity simulations will be used to calibrate FAST.Farm for a subset of cases, and FAST.Farm will be run many times to support the analysis required by the application.

Acknowledgements

The Alliance for Sustainable Energy, LLC (Alliance) is the manager and operator of the National Renewable Energy Laboratory (NREL). NREL is a national laboratory of the U.S. Department of Energy, Office of Energy Efficiency and Renewable Energy. This work was authored by the Alliance and supported by the U. S. Department of Energy under Contract No. DE-AC36-08GO28308. Funding was provided by the U.S. Department of Energy Wind Energy Technologies Office. The views expressed in the article do not necessarily represent the views of the U.S. Department of Energy or the U.S. government.The U.S. government retains and the publisher, by accepting the article for publication, acknowledges that the U.S. government retains a nonexclusive, paid-up, irrevocable, worldwide license to publish or reproduce the published form of this work, or allow others to do so, for U.S. government purposes.

References

[1] Jonkman J, Annoni J, Hayman G, Jonkman B and Purkayastha A 2017 Development of FAST.Farm: a new multiphysics engineering tool for wind-farm design and analysis *AIAA*

Science and Technology Forum and Exhibition (SciTech 2017), 9–13 January 2017, Grapevine (Dallas/Ft. Worth Region), TX [online proceedings] http://arc.aiaa.org/doi/pdf/10.2514/6.2017-0454

[2] Churchfield M J, Lee S, Moriarty P J, Martinez L A, Leonardi S, Vijayakumar G and Brasseur J G 2012 A large-eddy simulation of wind-plant aerodynamics *50th AIAA Aerospace Sciences Meeting Including the New Horizons Forum and Aerospace Exposition, 9–12 January 2012, Nashville, TN* [online proceedings] http://dx.doi.org/10.2514/6.2012-537

[3] Doubrawa P, Annoni J, Jonkman J and Ghate A 2018 Optimization-based calibration of FAST.Farm parameters against SOWFA *AIAA Science and Technology Forum and Exhibition (SciTech 2018), 8–13 January 2018, Kissimmee, FL* [online proceedings] https://arc.aiaa.org/doi/pdf/10.2514/6.2018-0512

[4] Churchfield M J, Moriarty P J, Hao Y, Lackner M A, Barthelmie R, Lundquist J and Oxley G S 2015 A comparison of the dynamic wake meandering model, large-eddy simulation, and field data at the Egmond aan Zee offshore wind plant *AIAA Science and Technology Forum and Exposition (SciTech 2015), 5–9 January 2015, Kissimmee, FL* [online proceedings] http://dx.doi.org/10.2514/6.2015-0724

[5] Larsen G C, Madsen H A, Thomsen K and Larsen T A 2008 Wake meandering: a pragmatic approach *Wind Energy* **11** pp 337-95 http://onlinelibrary.wiley.com/doi/10.1002/we.267/epdf

[6] Jonkman J, Butterfield S, Musial M and Scott G 2009 *Definition of a 5-MW reference wind turbine for offshore system development* NREL/TP-500-38060 (Golden: National Renewable Energy Laboratory) http://www.nrel.gov/docs/fy09osti/38060.pdf

[7] Quon E, Churchfield M and Jonkman J 2018 Comparison of wake characterization methods for large-eddy simulations of a rotor in stratified flow *Computers & Fluids* (Forthcoming)

[8] Martínez-Tossas L A, Churchfield M J and Meneveau C 2017 Optimal smoothing length scale for actuator line models of wind turbine blades based on Gaussian body force distribution *Wind Energy* **20** pp 1083-96 http://onlinelibrary.wiley.com/doi/10.1002/we.2081/epdf